



Full Text View

[Volume 29, Issue 6 \(June 1999\)](#)

Journal of Physical Oceanography

Article: pp. 1156–1165 | [Abstract](#) | [PDF \(146K\)](#)

Spume Drops Produced by the Wind Tearing of Wave Crests

Magdalena Anguelova, Richard P. Barber Jr. ^{*}, and Jin Wu ⁺*Air–Sea Interaction Laboratory, Graduate College of Marine Studies, University of Delaware, Lewes, Delaware*

(Manuscript received March 20, 1997, in final form June 10, 1998)

DOI: 10.1175/1520-0485(1999)029<1156:SDPBTW>2.0.CO;2

ABSTRACT

The wind tearing of breaking wave crests produces spume drops. The authors report preliminary laboratory data from direct and unambiguous observation of this process under various wind conditions using a video imaging technique. Results include the size distribution and production rates of these drops. The curves for production rates at different wind speeds merge effectively when normalized by the number of breaking events. This confirms that wave breaking occurrence, not the wind speed, is a dominant factor in spume production.

1. Introduction

Sea spray (marine aerosol) is involved in air–sea transfers of momentum, heat, and mass (Krauss 1967; Fairall et al. 1990; Blachard 1983; Eriksson 1959). Since the contribution of marine aerosols to these fluxes might be significant, Latham and Smith (1990) suggested sea spray as a probable negative feedback for global warming. This feedback is driven by the increased number of condensation nuclei in low clouds, whose influence on the planetary albedo is strong (Slingo 1990). In events such as hurricanes and frontal development, the latent heat flux is a major supplier of energy from ocean to atmosphere. Geernaert (1990) points out that for moderate to high wind speeds, the evaporation over the sea is dominated by foam and spray generated and entrained into the atmosphere by wind shearing and breaking waves. Fairall et al. (1994) ran a numerical model of tropical cyclones with wind velocities reaching 40 m s^{-1} , which showed that the contribution of sea spray to air–sea fluxes becomes comparable to direct fluxes of moisture and heat. In remote sensing, droplets are likely responsible for the deviations of radiometric (Black and Swift 1984) and scatterometric (Carswell et al. 1994) readings from model predictions starting at $15\text{--}20 \text{ m s}^{-1}$. This deviation cannot be accounted for by foam formation only. Tang (1974) made attempts to incorporate droplets into the radiometric algorithms.

Table of Contents:

- [Introduction](#)
- [Experiment](#)
- [Results](#)
- [Discussion](#)
- [Summary](#)
- [REFERENCES](#)
- [TABLES](#)
- [FIGURES](#)

Options:

- [Create Reference](#)
- [Email this Article](#)
- [Add to MyArchive](#)
- [Search AMS Glossary](#)

Search CrossRef for:

- [Articles Citing This Article](#)

Search Google Scholar for:

- [Magdalena Anguelova](#)
- [Richard P. Barber](#)
- [Jin Wu](#)

Current knowledge on sea spray, summarized by [Wu \(1982a, 1990a\)](#), [Blanchard \(1983\)](#), and [Andreas et al. \(1995\)](#), encompasses three important types of marine aerosols—film, jet, and spume drops—named after their production mechanisms. [Blanchard \(1963\)](#) presented data, and later [MacIntyre \(1972\)](#) considered the dynamics, of indirect formation of two types of these drops. When air bubbles burst at the water surface, film drops are generated from the shattering of the hemispherical bubble cap, while jet drops are produced when the bubble cavity collapses. [Andreas \(1992\)](#) summarized that film drops have typical diameters less than $5\ \mu\text{m}$, though [Resch et al. \(1986\)](#) sporadically measured film drops with radii up to $250\ \mu\text{m}$. The size of jet drops is considered by [Cipriano and Blanchard \(1981\)](#) to be about one-tenth that of the parent bubble with typical values in the range $3\text{--}100\ \mu\text{m}$ ([Andreas 1992](#)). Oceanic bubble population documented by [Kolovayev \(1976\)](#) with bubble trap device, and by [Johnson and Cooke \(1979\)](#) with a photographic system, show a maximum at about $100\ \mu\text{m}$, which implies a peak of jet drop concentration in the range $10\text{--}20\ \mu\text{m}$. Acoustical methods for sizing bubbles do not always reveal such a maximum in bubble distributions (e.g., [Medwin 1970](#); [Medwin and Breitz 1989](#)) and the issue of presence or absence of such a peak is debatable within the bubble community ([MacIntyre 1986](#); [Medwin and Breitz 1989](#)). Yet the measurements of [Cipriano and Blanchard \(1981\)](#) and [Mestayer and Lefauconnier \(1988\)](#) confirmed a maximum concentration of jet drops around $20\ \mu\text{m}$.

Spume drops are directly produced from the tearing of breaking wave crests by strong winds. Appearance of “foam streaks” along the direction of high winds was reported by [Ross and Cardone \(1974\)](#). [Bascom's \(1980\)](#) Table II listed the Beaufort scales for sea state description using “foam streaks aligned with the wind” as a characteristic feature. However, spume drops have usually drawn less attention as they were considered too large and heavy to stay above the sea surface for appreciable times in order to contribute to the exchange processes. Moreover, it is difficult to make reliable measurements in a “whole gale” ($\approx 25\ \text{m s}^{-1}$ wind) sea. Thus, spume drop observation has rarely been a deliberate goal in experiments, and their presence was only anticipated in early works ([Lai and Shemdin 1974](#); [Wang and Street 1978](#)). Recently, experimental findings have been more convincing. [Monahan et al. \(1983\)](#) observed a marked enhancement of the size spectrum at the large droplet end when winds reached 9 to $11\ \text{m s}^{-1}$ and attributed it to the production of droplets by surface tearing. The [Wu et al. \(1984\)](#) field experiment showed that the temporal distribution of drops in the lowest level of the atmosphere coincided with the wave period. Considering that a few wave periods are necessary for bubbles to rise and burst, this result suggested that film and jet drops could not be strongly correlated with the waves in time. Consequently, the observed periodicity in droplet distribution along the wave profile indicated further that the droplets are probably produced by tearing from the wave crests. Measuring the vertical profiles of large particles ($10\text{--}100\ \mu\text{m}$) above the sea surface, [de Leeuw \(1986\)](#) reported a maximum concentration around $1\text{--}2\ \text{m}$ elevation for a $12\ \text{m s}^{-1}$ wind. The occurrence of this maximum away from the sea surface was interpreted by [Wu \(1990b\)](#) as a production of droplets via tearing. The first experiment aimed at investigating the direct mechanism of drop production was that reported by [Koga \(1981\)](#) in a laboratory tank. Using a photographic technique of multicolored overlapping exposures, Koga observed small projections of water near the wave crests for a $14\text{--}16\ \text{m s}^{-1}$ wind. When these projections were fully developed and broke down, they produced droplets. Koga suggested that this description clarified the splashing mechanism of direct production of droplets. Judging by Koga's photographs and [Andreas et al.'s \(1995\)](#) drawing of the various kinds of sea spray droplets, Koga indeed observed splash drops (chop drops in terms of [Monahan et al. 1986](#) and [Woolf et al. 1987](#)). These splash drops, though produced directly, differ from spume drops by the mechanism of formation, number, and significance in oceanographic processes. Thus, [Koga's \(1981\)](#) study probably remains the most complete study of splash drops and marks the beginning of study of various direct mechanisms of producing drops. While [Koga and Toba \(1981\)](#) reported droplets produced by direct mechanisms larger than $550\ \mu\text{m}$, [Andreas \(1992\)](#) suggested that the initial radius of a spume drop may be as small as $20\ \mu\text{m}$.

[Monahan et al. \(1986\)](#) proposed the first model accounting for the production of spume drops with increasing wind speed. They expanded the expression for the sea spray source (or generation) function, which quantified the rate of production of indirectly (film and jet) produced drops, with a term predicting the number and size of directly produced spume drops. [Andreas \(1992\)](#), [Wu \(1993\)](#), and [Andreas et al. \(1995\)](#) further refined the wind speed dependence of the spume drop production. A workshop summary ([Goroch and Geernaert 1995](#)) recognized the importance of the source function and pointed out uncertainties of three orders of magnitude in its determination.

Despite their obvious significance at high winds, the size and vertical distributions of spume drops are practically unknown. [Fairall et al. \(1994\)](#), [Andreas et al. \(1995\)](#), and [Goroch and Geernaert \(1995\)](#) conclude that a major limitation for further theoretical investigations and complete parameterization of the spume drop component of marine aerosol remains the lack of direct observations. As field measurements of such a phenomenon are rather difficult, a laboratory study to observe and quantify spume drop production is reported here.

2. Experiment

a. Previous techniques

Various experimental techniques have been used in jet and film drop investigations. Not surprisingly, one ideal technique cannot be pointed out considering issues such as size range coverage, reliability, efficiency, and tractability to automated processing. Collection methods, used by [Woodcock \(1953 1972\)](#), [Preobrazhenskii \(1973\)](#), [Lovett \(1978\)](#), [Koga and Toba](#)

(1981), [Blanchard et al. \(1984\)](#), and [de Leeuw \(1986\)](#) are straightforward in principle, especially in field measurements under moderate winds (up to 10 m s^{-1}). However, their application to extreme field conditions is certainly not easy, and the processing of the sample plates seems laborious. The tediousness in processing data was considered the main drawback of the early photographic systems, employed by [Toba \(1961\)](#), [Blanchard \(1963\)](#), [Monahan \(1968\)](#), and [Koga and Toba \(1981\)](#). Electrical sensors, used by [Lai and Shemdin \(1974\)](#), [Wang and Street \(1978\)](#), and [Spiel \(1995\)](#), are another possibility for sampling droplets, but their effectiveness is usually limited by the small sensing area. Also, to avoid contamination of data from high waves, electric sensors cannot be placed close enough to the water surface, say in the wave trough. This problem would probably render measurements under high wind conditions almost impossible. [Woodcock et al. \(1953\)](#), [Wu \(1973, 1977\)](#), [Schacher et al. \(1981\)](#), [Cipriano and Blanchard \(1981\)](#), [Wu et al. \(1984\)](#), [Resch et al. \(1986\)](#), [Resch and Afeti \(1991, 1992\)](#), [Mestayer and Lefauconnier \(1988\)](#), and [Spiel \(1995\)](#) used different types of optical devices. These possess many advantages, including no disturbance of the flow, placing the light beam at different sites, large sensing volume, and easy data processing. However, it is difficult to cover a wide size range, for example, from film to spume drops. Obviously, the choice of the system depends on the goal pursued. The feasibility of a standard video imaging technique for direct detection of the production of spume drops is tested in the present study.

b. Equipment and experimental conditions

Experiments were performed in the Wind–Wave–Current Research Facility in the Air–Sea Interaction Laboratory. The tank is 37 m long and 1 m wide; the water depth is 0.75 m, and the wind tunnel is 0.55 m high. Front and back side walls of the tank are transparent. A 1000-W light source was supported above the tank to shine vertically downward through an opening in the tank cover. The cross section of the illuminated area at the still water surface had dimensions of 13 cm across and 38 cm along the tank. A standard CCD camera, located perpendicularly to the wall of the tank, captured the production of spume drops in a field of view (FOV) extending 20.5 cm along the tank and 15.5 cm vertically. This FOV was offset to 6 cm from the still water level, which was enough to catch the tip of the wave crests but to avoid “filling” the FOV with water at high wind speeds. With a distance of 1 m from the camera to the tank wall, the resolution for particle sizing was 0.27 and 0.65 mm in horizontal and vertical directions, respectively. A shutter speed of 1 ms effectively froze the motion of slower (generally larger) drops, with faster (generally smaller) ones typically appearing as streaks.

The wind speeds for the onset of spume drop production reported in the literature are summarized by [Andreas et al. \(1995\)](#). On the basis of mostly field experiments these authors prefer to accept a wider range of wind speeds ($7\text{--}11 \text{ m s}^{-1}$) than usually believed (at least 9 m s^{-1}). In a laboratory study [Mestayer and Lefauconnier \(1988\)](#) expected production of spume drops at wind speeds higher than 9 m s^{-1} . In our Air–Sea Interaction Laboratory, spume drops start to appear occasionally at winds of 9 m s^{-1} . Since the main goal of the present study was the direct observation of the process of spume drop production rather than a systematic parameterization, only four wind velocities were used ([Table 1](#)). These reference wind speeds, U , were measured and controlled with a Pitot tube positioned in the undisturbed airflow above the water surface. Once adjusted, the wind speed showed a remarkable stability according to the frequent readings of the Pitot tube. The reference values of the wind speed were converted to U_{10} values in order to compare the results with the existing models. The calculations used the set of equations ([Wu 1968, 1980](#))

$$U_{10} = U + \left(\frac{u_*}{k} \right) \ln \left(\frac{10}{z} \right)$$

$$u_*^2 = C_{10} U_{10}^2$$

$$C_{10} = (0.8 + 0.065 U_{10}) \times 10^{-3},$$

where U is the reference wind speed measured at height $z = 0.28 \text{ m}$, $k = 0.4$ the von Kármán constant, u_* the friction velocity, and C_{10} the wind stress coefficient. The U_{10} values for the corresponding reference values are listed in [Table 1](#).

c. Data processing procedures

Three-minute video records were made with a video cassette recorder. Only the frames containing events of breaking waves accompanied with torn drops were digitized and further analyzed using image analysis software. With a frame rate of 30 Hz, such events were observed in roughly 3% of the total 5400 frames at $U = 11 \text{ m s}^{-1}$ and in about 12% of the frames at $U = 14 \text{ m s}^{-1}$ wind. The number of drops was counted in all digitized images and their positions, that is, horizontal and vertical coordinates, and sizes were extracted. Note that if multiple images were available from one breaking wave, drops were counted only in one or every other image to avoid repeat counting. The number of digitized images and total number of

drops for each wind speed counted from them are summarized in [Table 1](#). We believe the obtained number of drops is large enough for reliable statistics of the drops sizes and rate of production.

The ellipticity of large drops, such as the spume drops with diameters above 3–4 mm, is an intrinsic characteristic as [Clift et al. \(1978\)](#) pointed out. Hence, the most rigorous way to determine the drop sizes is to calculate an equivalent diameter following the procedure used by [Kalvoda \(1992\)](#): the area of an ellipse ($=\pi xy/4$, where x and y are the measured horizontal and vertical major axes) is set equal to the area of a circle ($=\pi d^2/4$) and an equivalent diameter is calculated by $d = (xy)^{1/2}$. Initially we calculated the diameters of the spume drops using this formula. Note, however, that the smaller spume drops are more spherical (with nearly equal values for horizontal and vertical axes) than the large ones which display stronger ellipticity. These smaller spume drops appeared to be additionally elongated because of their fast motion. Since the smaller drops appear more frequently in our measurements, the error introduced by image smearing due to horizontal motion is larger than the error due to neglecting the ellipticity. Therefore, the diameter was derived from the vertical dimension only. This approach involves a slight underestimation of the size of the drops. Also note that at the working resolution of the system the focusing depth was smaller than the width of the illuminated area across the tank (13 cm). Therefore, we often do observe drops that are slightly out of focus. This adds a systematic overestimation of the drop sizes, which outweighs the underestimation caused by neglecting the ellipticity. Generally, the effect of small focusing depth can be either avoided by confining the observations within the focus depth dimension or accounted for with a proper processing algorithm. The former approach would result in the counting of fewer drops, thus affecting the reliability of the size distributions. We chose not to pursue the latter approach since the main purpose of the study was to determine the production rate of spume drops rather than their precise sizing. Thus, for now the bias of all sizes toward larger values is only noted.


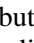
Once the total number of droplets for the 3-min time span was counted and their diameters calculated, the size distribution, in μm^{-1} , was constructed. The resolution of the technique (about $650 \mu\text{m}$ in the vertical direction) led to the division of the diameter axis into 18 equal increments, covering a range from 0 to 12 mm in bands of 0.66 mm. Normalizing the size distributions with the time interval (3 min) and the area of illuminated water surface within the FOV of the camera ($2.7 \times 10^{-2} \text{ m}^2$), the production rate per unit time per unit area in a size band ($\text{s}^{-1} \text{ m}^{-2} \mu\text{m}^{-1}$) was obtained. The dimensions of the illuminated water surface were chosen to be the length of the FOV along the tank (20.5 cm) and the length of the illuminated water surface across the tank (13 cm).


The vertical positions of the drops above the water surface were calculated by adding their vertical coordinates, registered within the 15-cm vertical dimension of the FOV, and the offset of 6 cm above the still water surface (see [section 2b](#)). Using these drop heights the vertical distributions were calculated. Though adequate, our setup is not optimal for registering the vertical distributions: we do not see the wave profile in our images and we miss the possible drops above the FOV. Thus, our vertical distributions are probably incomplete and we report the vertical position of the drops relative to still water level, while their position relative to the wave profile is more desirable. Drop velocities were obtained in two ways. First, the displacement of a drop from one video frame to another in a time interval of 33 ms was used. A difficulty with this procedure was achieving the unambiguous identification of the same drop in consecutive frames. No more than 20 drops for a given wind speed were found useful for this procedure. In the second approach, the horizontal smearing of a drop ($=x - y$) during the open shutter time ($=1 \text{ ms}$) was used. The wide scatter of results for the drop velocity proved that the number of tracked drops in both procedures was too small for good statistics. We will, therefore, concentrate on the results of spume drop production rates.

3. Results

The process of spume drop production is unambiguously captured in [Fig. 1](#). In [Fig. 1a](#), the FOV of the camera is larger than that used for analysis (of course, at the expense of resolution) in order to show the process of drop tearing together with the breaking wave crest. The image in [Fig. 1b](#) gives an example of torn drops in the actual FOV.

Quantitative results for the size distribution and rate of spume drop production at various wind velocities are plotted in [Fig. 2](#). [Figure 2a](#) shows the distributions of the absolute values of all counted drops by size, and [Fig. 2b](#) gives the rate of production of spume drops in $\mu\text{m}^{-1} \text{ s}^{-1} \text{ m}^{-2}$. The apparent peaks in the production rates for 13 and 14 m s^{-1} winds near 2 mm are primarily due to equipment resolution, limiting a reliable detection of the smallest drops at these winds. This cutoff for small diameters is accentuated by the increase in production of large drops at high winds. With one exception, we do not observe drops smaller than approximately $900 \mu\text{m}$, though the system allows the detection of sizes down to $650 \mu\text{m}$. The reason is the already discussed issue of the small focusing depth. The production rate is highest for the drops in the size range of 0.7–4 mm and negligible for those $>8 \text{ mm}$ even at 14 m s^{-1} winds. As expected, with an increase of the wind velocity, and hence in the frequency of occurrence of wave breaking, the production of drops increases. The normalization of the production rate with the number of breaking events, counted visually from the records and including both events with and without spume drops, effectively merges the curves for the different winds, [Fig. 2c](#), proving the strong correlation between the processes of wave breaking and drop generation.



These conclusions do not change significantly if a 1-min interval (1800 total frames) of data is considered instead of the full 3 min. The absolute numbers of counted drops goes down by a factor between 2 and 3, as shown by the open circles in [Fig. 3](#) , but the shape of the size distributions and the place of the maximum production rate remain the same for all four winds. This fact confirms the statistical validity of the results. On the other hand, the production of spume drops is an inherently “patchy” process both spatially and temporally, and arbitrarily short sampling times are therefore not appropriate. The normalization of the curves in [Fig. 3](#)  with the corresponding time interval (60 or 180 s) merges them only approximately, which points out the temporal nonstationarity of the process of spume drop generation.

Spume drops were observed at elevations as high as 21 cm above the still water surface. The horizontal velocity of the drops ranged from 1.5 to 5.4 m s⁻¹. A slight dependence on wind velocity was manifested as broadening of the range toward higher values at higher winds. No clear dependence of the drop velocity on the drop size was revealed. Closer observation of the images showed occasional disruption or coalescence of water particles. Disruption of a chunk of water into several smaller drops from the fast motion is marked in [Fig. 4](#)  with ellipses.

4. Discussion

With the capabilities of a standard camera we count relatively large drops, while the sizes less than about 650 μm are not accessible. Consequently, the reported results show the contribution of the direct tearing mechanism to the large-size end of the drop size spectrum. The observation of such drop sizes is consistent with [Koga and Toba's \(1981\)](#) measurements of directly produced drops. The trend of the curves, however, implies that the spume drop production is probably more abundant at smaller diameters, in accordance with previous suggestions ([Andreas 1992](#)). Further investigations over smaller sizes are necessary.

Are the observed drops only spume drops or are spume drops mixed with jet and film drops? [Woolf et al. \(1987\)](#) discussed four properties that distinguish film and jet drops. These were the time of production relative to the moment of wave breaking, the site of production relative to the active whitecap plume, electrostatic charge per drop, and the dependence of the number of drops produced on the water temperature. They investigated all of these properties except the site of production. [Cipriano and Blanchard's \(1981\)](#) study offered another possibility for the partition of film and jet drops. As the number of jet and film drops depends on the diameter of the parent bubble, the shape of the bubble size distribution is critical for the relative contribution of each type of drop. Bubbles larger than 1.8 mm produce more film drops than jet drops and vice versa ([Resch and Afeti 1991](#)). Can these conclusions be used for the separation of jet and/or film drops from spume drops? We believe that speculations about the time, site, and size of the drops generated are only partially valid. As a function of time, the first drops produced would be spume drops, followed by film and finally jet drops. However, since the spume drops fly ahead of the wave crest, they would be mixed with the film and jet drops produced by the preceding crest. Speculations about the site of production (the crest or the trough of the wave) of different drops, aided by reliable vertical distributions relative to the wave profile, are similar. [Wu's \(1990b\)](#) interpretation of the [de Leeuw \(1986\)](#) results on vertical profiles of giant particles established the wave height as a reliable means for distinguishing spume from jet drops. The former would be related to the wave crest, hence will be situated higher, while the latter would be confined mostly in the wave trough. However, the height of the drops over the water surface is not always applicable for the separation of film and spume drops since the film drops are also related to the active whitecap plume ([Woolf et al. 1987](#)). The aforementioned typical drop sizes suggest that confident separation by drop size is possible only for very small and very large drops. It is almost certain that drops smaller than 20 μm are not spume drops and those larger than 550 μm are not jet or film drops. We support the idea expressed by [Koga \(1981\)](#) that it is quite possible that all three types of drops exist simultaneously in the range of 50–500 μm. In an experiment dealing with these sizes the separation of the relative number of different types of drops would be very complicated. For the case in hand, the inability to detect drops below approximately 650 μm gives the assurance that mainly spume drops were observed.

The wind dependence of the total production rate, $P_t(U_{10})$, of drops of all types (film, jet, and spume) and sizes was estimated in models by [Monahan et al. \(1986\)](#), [Andreas \(1992\)](#), and [Wu \(1993\)](#). In [Fig. 5](#)  those (solid symbols) are compared with the present observations (open circles) of only spume drops, that is, the drops with the largest possible sizes. The U_{10} values instead of the measured reference wind values were used. Two laws were fitted to the present data: power and exponential laws in the forms $P_t = aU_{10}^b$ and $P_t = a \exp(bU_{10})$, respectively. Judging by the various statistics of the fittings, the exponential law with coefficients $a = 1.1$ and $b = 0.23$ was chosen. The solid line in [Fig. 5](#)  for winds from 7 to 30 m s⁻¹ was plotted using these coefficients. It is seen that the trend of the production rate with wind speed is similar to that of [Andreas \(1992\)](#) (triangles), but with values two orders of magnitude lower. This is understandable as only relatively large drops were counted in the present experiment and the bulk of smaller ones, of whatever type, is not included. Yet, the fit is useful in speculating on the contribution of spume drops alone: there is at most one drop per unit area per unit time at the onset of spume drop production (7 m s⁻¹) and a thousand drops per unit area per unit time for storm conditions (30 m s⁻¹).

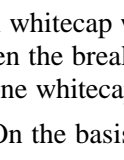
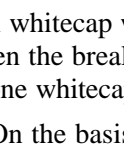
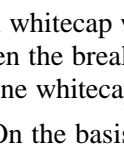
Because the intensive production of spume drops occurs under strong winds, it is difficult to imagine field investigations, unless “revolutionary droplet measuring technology” is devised as [Andreas et al. \(1995\)](#) noted. Approaches to estimating spume drop production that involve merely measuring the wind velocity are therefore valuable. The exponential law, derived from fitting the data, makes it possible to estimate the total number of drops produced in a unit time by a unit area knowing U_{10} :

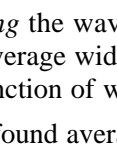
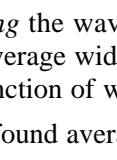
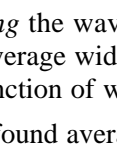
$$P_t = 1.1e^{0.23U_{10}}.$$

Another approach to connecting laboratory and field measurements is to find a “field” parameter obtainable from the measurement of wind speed, and having a similar parameter from the laboratory to calculate a rescaling factor. This factor applied to laboratory data for the production rate P would give us an estimate for the production rate in the field P_{field} . Thus, we propose the parameter breaking crest length L .

The term “breaking crest length” was defined by [Phillips \(1985\)](#) as the total length L of all breaking crests w_i in a unit area A ,

$$L = \sum_{i \in A} w_i,$$

[Fig. 6](#) . On a scale of an individual whitecap we consider that the whitecap width w (along the wave crest, [Fig. 6](#) ) represents the breaking crest length. Then the breaking crest length can be expressed as the average width of a whitecap divided by the average area containing one whitecap, A_0 , or $L = w/A_0$. To determine L as a function of wind velocity we need to find expressions for \bar{w} and A_0 . On the basis of [Bortkovskii's \(1987\)](#) data, [Wu \(1992\)](#) found averaged values for whitecap width \bar{w} and whitecap length \bar{l} (across the breaking crest, [Fig. 6](#) ) and introduced three relations: aspect ratio of an individual whitecap $\bar{w}/\bar{l} = 2.15$; a characteristic length scale for an individual whitecap $s = (\bar{w}/\bar{l})^{1/2}$; and wind dependence of s , $s = 0.335U_{10}^{0.8}$. Employing these three relations we can write $\bar{w} = 0.491U_{10}^{0.8}$. Using the characteristic length scale s and A_0 , we may write down the whitecap coverage due to an individual whitecap as $W = s^2/A_0$. In addition, [Wu \(1988\)](#) proposed an expression for wind speed dependence of W , $W \propto U_{10}^{3.75}$, where W is in ppm. [Monahan and O'Muircheartaigh \(1982\)](#) acknowledged that, if a formula providing a simple estimation of oceanic whitecap coverage from the 10-m wind speed is necessary, any of the several proposed dependencies ([Wu 1982b](#); [Monahan and O'Muircheartaigh 1982](#)) can be accepted with only slightly worse values than those obtained with ordinary least square fitting used by them ([Monahan and O'Muircheartaigh 1980](#)). So, we obtain $A_0 = 5.6 \times 10^4 U_{10}^{-2.15}$. Now, combining \bar{w} and A_0 we obtain an expression for breaking crest length as a function of wind speed U_{10} : $L = 8.77 \times 10^{-6} U_{10}^{2.95}$. From field measurements of the wind, the total breaking crest length per unit sea surface area can be determined, $L_{\text{field}}(U_{10})$ (in m m^{-2}). Then, having laboratory production data, P (in $\text{s}^{-1} \text{m}^{-2}$), normalized with breaking crest length L_{lab} (m m^{-2}), normalized production rate, P_{lab} (in $\text{s}^{-1} \text{m}^{-1}$), can be obtained and used for estimation of field production as $P_{\text{field}} = L_{\text{field}}(U_{10}) \times P_{\text{lab}}$ (in $\text{s}^{-1} \text{m}^{-2}$).

Application of this concept to our measurements should be approached with caution. We can estimate P_{field} and compare these with the model results in [Fig. 5](#)  using our measurements and the expression $P_{\text{field}} = L(U_{10}) \times P_{\text{lab}}$. One must realize, however, that since $L_{\text{field}}(U_{10})$ gives different length scales (factors) for different winds, P_{lab} should be obtained by normalizing with length scales L_{lab} corresponding to different winds in the tank too. While the calculation of four values of $L_{\text{field}}(U_{10})$ is straightforward, we do not have auxiliary measurements to provide correct $L_{\text{lab}}(U_{10})$ values. What we can use from the present setup are the length scales of the FOV across the tank ($w = 13 \text{ cm}$) and the illuminated area 2.7×10^{-2} as A_0 . That is, we have only one value for $L_{\text{lab}} = 0.13/(2.7 \times 10^{-2})$ for all four production cases. However, the good scaling of production rate with breaking crest length shown in [Fig. 2c](#)  suggests that this approximation may only weakly affect the results. With this precautionary note we plot our estimated field production rate in [Fig. 5](#)  (open squares). The rescaling of the laboratory values yields to lower production rates in the field for the large drop sizes measured in this study.

5. Summary

Direct measurements of spume drops produced by the wind tearing of wave crests have been made. The principal advantage of the photographic technique employed is the unambiguous observation of the production mechanism.

Statistically sound preliminary data on the distribution of total numbers of drops and the production rate, in $\mu\text{m}^{-1} \text{s}^{-1} \text{m}^{-2}$, of spume drops are presented. Results indicate that rather large drops, up to 10 mm, can be formed in this process and contribute to the large-size end of the size spectrum of sea spray. Indirectly produced film and jet drops are not accessible with the reported experimental setup, which ensures that mainly spume drops are observed. An exponential law fits the production of spume drops with increasing wind velocity and provides a means for obtaining the production rate as a function of the wind velocity. A concept for estimation of spume drop production in the field using laboratory data normalized with breaking crest length is proposed.

The photographic technique used is adequate for direct and unambiguous measurements of the process of drops tearing from the wave crests. Unfortunately, the spatial resolution of a standard camera is not enough to resolve drops below 650 μm , and an optical system with small focusing depth further introduces an overestimation of drop sizes. These, however, are not overwhelming disadvantages in the present study for two reasons: 1) reliable separation of the large spume drops from the jet and film drops is assured and 2) the spume drops contribute significantly to the large-size end of the drop-size spectrum. Cameras with better resolution are available, and a similar study over smaller sizes is feasible. Problems that should be addressed in such an experiment would be the partition of the different types of drops and accounting for the focusing depth effect. A fast motion camera is the correct choice for investigating drop velocities and trajectories. Note, however, that high time-resolution cameras generally suffer low spatial-resolution. The analysis of many drops in many digitized images can be automated and sped up through specialized image processing packages. Measurements of spume drop characteristics using a video imaging technique have proven feasible and a systematic parameterization of spume drop production is the next necessary step.

Acknowledgments

We gratefully acknowledge technical support from Mr. M. Wo and fruitful discussions with Drs. A. Savtchenko and S. Tang. We are also pleased to thank Mr. P. Vagenas and the Theater Department for the loan of their spotlight. The constructive critique of two anonymous reviewers is highly appreciated.

REFERENCES

- Andreas, E. L., 1992: Sea spray and the turbulent air-sea heat fluxes. *J. Geophys. Res.*, **97**, 11 429–11 441..
- , J. B. Edson, E. C. Monahan, M. P. Rouault, and S. D. Smith, 1995: The spray contribution to the net evaporation from the sea: A review of recent progress. *Bound.-Layer Meteorol.*, **72**, 3–52..
- Bascom, W., 1980: *Waves and Beaches: Dynamics of the Ocean Surface*. Anchor Press, 353 pp..
- Black, P. G., and C. L. Swift, 1984: Airborne stepped frequency microwave radiometer measurements of rainfall rate and surface wind speed in hurricanes. *Proc. 22d Conf. on Radar Meteorology*, Zurich, Switzerland, Amer. Meteor. Soc., 433–438..
- Blanchard, D. C., 1963: The electrification of the atmosphere by particles from bubbles in the sea. *Progress in Oceanography*, Vol. 1, Pergamon, 71–202..
- , 1983: The production, distribution and bacterial enrichment of the sea-salt aerosol. *Air-Sea Exchange of Gases and Particles*, P. S. Liss and W. G. N. Slinn, Eds., D. Reidel, 407–454..
- , A. H. Woodcock, and R. J. Cipriano, 1984: The vertical distribution of the concentration of sea salt in the marine atmosphere near Hawaii. *Tellus*, **36B**, 118–125..
- Bortkovskii, R. S., 1987: *Air-Sea Exchange of Heat and Moisture During Storms*. E. C. Monahan, Ed., D. Reidel, 194 pp..
- Carswell, J. R., S. C. Carson, R. E. McIntosh, F. K. Li, G. Neumann, D. J. McLaughlin, J. C. Wilkerson, P. G. Black, and S. V. Nghiem, 1994: Airborne scatterometers: Investigating ocean backscatter under low- and high-wind conditions. *Proc. IEEE*, **82**, 1835–1860..
- Cipriano, R. J., and D. C. Blanchard, 1981: Bubble and aerosol spectra produced by a laboratory “breaking wave.” *J. Geophys. Res.*, **86**, 8085–8092..
- Clift, R., J. R. Grace, and M. E. Weber, 1978: *Bubbles, Drops, and Particles*. Academic Press, 380 pp..
- de Leeuw, G., 1986: Vertical profiles of giant particles close above the sea surface. *Tellus*, **38B**, 51–61..
- Eriksson, E., 1959: The yearly circulation of chloride and sulfur in nature: Meteorological, geochemical and pedological implications. Part I. *Tellus*, **11**, 375–403..

Fairall, C. W., J. B. Edson, and M. A. Miller, 1990: Heat fluxes, whitecaps, and sea spray. *Surface Waves and Fluxes*, Vol. 1, G. L. Geernaert and W. J. Plant, Eds., Kluwer Academic, 173–208..

—, J. D. Kepert, and G. J. Holland, 1994: The effect of sea spray on surface energy transports over the ocean. *Global Atmos. Ocean Sys.*, **2**, 121–142..

Geernaert, G. L., 1990: Bulk parameterization for the wind stress and heat fluxes. *Surface Waves and Fluxes*, Vol. 1, G. L. Geernaert and W. J. Plant, Eds., Kluwer Academic, 91–172..

Goroch, A. K., and G. Geernaert, Eds., 1995: *Coastal Aerosol Workshop Proceedings*. 142 pp..

Johnson, B. D., and R. C. Cooke, 1979: Bubble populations and spectra in coastal waters: A photographic approach. *J. Geophys. Res.*, **84**, 3761–3766..

Kalvoda, P. M., 1992: Macrobubble clouds produced by breaking wind waves. M.S. thesis, Graduate College of Marine Studies, University of Delaware, 80 pp..

Koga, M., 1981: Direct production of droplets from breaking wind-waves—Its observation by a multicolored overlapping exposure photographing technique. *Tellus*, **33**, 552–563..

—, and T. Toba, 1981: Droplet distribution and dispersion processes on breaking wind waves. *Tohoku Geophys. J.*, **28**, 1–25..

Kolovayev, P. A., 1976: Investigation and statistical size distribution of wind produced bubbles in the near-surface ocean layer. *Oceanol.*, **15**, 659–661..

Krauss, E. B., 1967: Wind stress along the sea surface. *Advances in Geophysics*, Vol. 12, Academic Press, 213–255..

Lai, R. J., and O. H. Shemdin, 1974: Laboratory study of the generation of spray over water. *J. Geophys. Res.*, **79**, 3055–3063..

Latham, J., and M. H. Smith, 1990: Effect on global warming of wind-dependent aerosol generation at the ocean surface. *Nature*, **347**, 372–373..

Lovett, R. F., 1978: Quantitative measurement of airborne sea-salt in the North Atlantic. *Tellus*, **30**, 358–363..

MacIntyre, F., 1972: Flow patterns in breaking bubbles. *J. Geophys. Res.*, **77**, 5211–5228..

—, 1986: On reconciling optical and acoustical bubble spectra in the mixed layer. *Oceanic Whitecaps and Their Role in Air–Sea Exchange Processes*, E. C. Monahan and G. M. Niocaill, Eds., D. Reidel, 75–94..

Medwin, H., 1970: In situ acoustic measurements of bubble populations in coastal ocean waters. *J. Geophys. Res.*, **75**, 599–611..

—, and N. D. Breitz, 1989: Ambient and transient bubble spectral densities in quiescent seas and under spilling breakers. *J. Geophys. Res.*, **94**, 12 751–12 759..

Mestayay, P., and C. Lefauconnier, 1988: Spray droplet generation, transport, and evaporation in a wind wave tunnel during the Humidity Exchange over the Sea Experiment in the Simulation Tunnel. *J. Geophys. Res.*, **93**, 572–586..

Monahan, E. C., 1968: Sea spray as a function of low elevation wind speed. *J. Geophys. Res.*, **73**, 1127–1137..

—, and I. G. O’Muircheartaigh, 1980: Optimal power-law description of oceanic whitecap coverage dependence on wind speed. *J. Phys. Oceanogr.*, **10**, 2094–2099.. [Find this article online](#)

—, and —, 1982: Reply. *J. Phys. Oceanogr.*, **12**, 751–752.. [Find this article online](#)

—, C. W. Fairall, K. L. Davidson, and P. Jones-Boyle, 1983: Observed inter-relations between 10 m winds, ocean whitecaps, and marine aerosols. *Quart. J. Roy. Meteor. Soc.*, **109**, 379–392..

—, D. E. Spiel, and K. L. Davidson, 1986: A model of marine aerosol generation via whitecaps and wave disruption. *Oceanic Whitecaps and Their Role in Air–Sea Exchange Processes*, E. C. Monahan and G. M. Niocaill, Eds., D. Reidel, 167–174..

Phillips, O. M., 1985: Spectral and statistical properties of the equilibrium range in wind-generated gravity waves. *J. Fluid Mech.*, **156**, 505–531..

Preobrazhenskii, L. Yu., 1973: Estimate of the content of spray-drops in the near-water layer of the atmosphere. *Fluid Mech. Sov. Res.*, **2**, 95–100..

Resch, F. J., and G. M. Afeti, 1991: Film drop distributions from bubbles bursting in seawater. *J. Geophys. Res.*, **96**, 10 681–10 688..

— ,and — ,1992: Submicron film drop production by bubbles in sea water. *J. Geophys. Res.*, **97**, 3679–3683..

— ,J. S. Darrozes, and G. M. Afeti, 1986: Marine liquid aerosol production from bursting of air bubbles. *J. Geophys. Res.*, **91**, 1019–1029..

Ross, D. B., and V. Cardone, 1974: Observation of oceanic whitecaps and their relation to remote measurements of surface wind speed. *J. Geophys. Res.*, **79**, 444–452..

Schacher, G. E., K. L. Davidson, C. W. Fairall, and D. E. Spiel, 1981: Calculation of optical extinction from aerosol spectral data. *Appl. Opt.*, **20**, 3951–3957..

Slingo, A., 1990: Sensitivity of the Earth's radiation budget to changes in low clouds. *Nature*, **343**, 49–51..

Spiel, D. E., 1995: On the birth of jet drops from bubbles bursting on water surface. *J. Geophys. Res.*, **100**, 4995–5006..

Tang, C. C. H., 1974: The effect of droplets in the air–sea transition zone on the sea brightness temperature. *J. Phys. Oceanogr.*, **4**, 579–593.. [Find this article online](#)

Toba, Y., 1961: Drop production by bursting of air bubbles on the sea surface, III, Study by use of wind flume. *Mem. Coll. Sci. Univ. Kyoto, Ser. A*, **29**, 313–344..

Wang, C. S., and R. L. Street, 1978: Measurements of spray at an air–water interface. *Dyn. Atmos. Oceans*, **2**, 141–152..

Woodcock, A. H., 1953: Salt nuclei in marine air as a function of altitude and wind force. *J. Meteor.*, **10**, 362–371..

— ,1972: Smaller salt particles in oceanic air and bubble behavior in the sea. *J. Geophys. Res.*, **77**, 5316–5321..

— ,C. F. Kientzler, A. B. Arons, and D. C. Blanchard, 1953: Giant condensation nuclei from bursting bubbles. *Nature*, **172**, 1144–1145..

Woolf, D. K., P. A. Bowyer, and E. C. Monahan, 1987: Discriminating between the film drops and jet drops produced by a simulated whitecap. *J. Geophys. Res.*, **92**, 5142–5150..

Wu, J., 1968: Laboratory studies of wind–wave interactions. *J. Fluid Mech.*, **34**, 91–112..

— ,1973: Spray in the atmospheric surface layer: Laboratory study. *J. Geophys. Res.*, **78**, 511–519..

— ,1977: Fast-moving suspended particles: Measurements of their size and velocity. *Appl. Opt.*, **16**, 596–600..

— ,1980: Wind-stress coefficients over sea surface near neutral conditions—A revisit. *J. Phys. Oceanogr.*, **10**, 727–740.. [Find this article online](#)

— ,1982a: Sea spray—A further look. *J. Geophys. Res.*, **87**, 8905–8912..

— ,1982b: Comment on “Optimal power-law description of oceanic whitecap coverage dependence on wind speed.” *J. Phys. Oceanogr.*, **12**, 750–751.. [Find this article online](#)

— ,1988: Variations of whitecap coverage with wind stress and water temperature. *J. Phys. Oceanogr.*, **18**, 1448–1453.. [Find this article online](#)

— ,1990a: On parameterization of sea spray. *J. Geophys. Res.*, **95**, 18 269–18 279..

— ,1990b: Vertical distribution of spray droplets near the sea surface: Influence of jet drop ejection and surface tearing. *J. Geophys. Res.*, **95**, 9775–9778..

— ,1992: Individual characteristics of whitecaps and volumetric description of bubbles. *IEEE Trans. Oceanic Eng.*, **17**, 150–158..

— ,1993: Production of spume drops by the wind tearing of wave crests: The search for quantification. *J. Geophys. Res.*, **98**, 18 221–18 227..

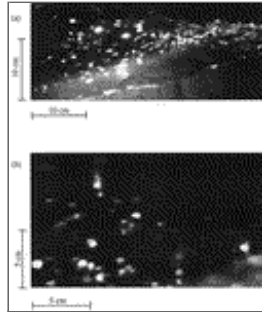
— ,J. J. Murray, and R. J. Lai, 1984: Production and distribution of sea spray. *J. Geophys. Res.*, **89**, 8163–8169..

Table 1. Summary of experimental quantities.

Reference wind speed U (m s^{-1})	Wind speed U_{10} (m s^{-1})	Number of useful images	Number of total drops counted
11.4	18.3	184	236
12.2	20.4	357	522
13.1	22.7	551	1124
14.1	25.0	643	1567

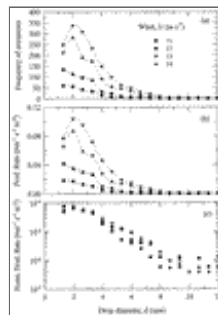
[Click on thumbnail for full-sized image.](#)

Figures



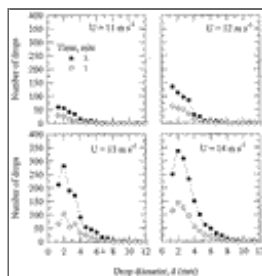
[Click on thumbnail for full-sized image.](#)

Fig. 1. Video images of spume drop production, in large field of view (FOV) with shutter speed of 2 ms (a), and in the actual FOV used for analysis, shutter speed 1 ms (b). Wind speed of 13 m s^{-1} is from right to left.



[Click on thumbnail for full-sized image.](#)

Fig. 2. Spume drop size distribution (a), production rate (b), and production rate normalized with the number of breaking events (c).



[Click on thumbnail for full-sized image.](#)

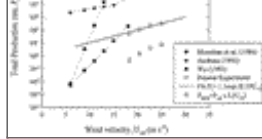
Fig. 3. Spume drops size distribution for different time intervals at different wind speeds.



[Click on thumbnail for full-sized image.](#)

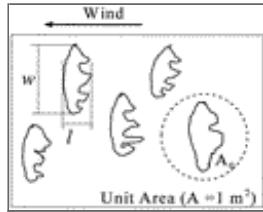
Fig. 4. Illustration of drop disruption (marked with ellipses).





Click on thumbnail for full-sized image.

Fig. 5. Comparison of the experimental and estimated data with previous models. The data are fitted with an exponential law; the coefficients are shown in the legend.



Click on thumbnail for full-sized image.

Fig. 6. A schematic of a unit area of sea surface containing whitecaps. The whitecap width (along the wave crest, hence across wind direction) and the whitecap length (across the wave crest, hence along wind direction) are shown. A_0 is the average area containing one whitecap.

* Current affiliation: Department of Physics, Santa Clara University, Santa Clara, California.

+ Current affiliation: Institute of Hydraulic and Ocean Engineering, National Cheng Kung University, Tainan, Taiwan, Republic of China.

Corresponding author address: Ms. Magdalena Anguelova, College of Marine Studies, University of Delaware, 700 Pilottown Road, Lewes, DE 19956.

E-mail: magde@udel.edu

top ▲



© 2008 American Meteorological Society [Privacy Policy and Disclaimer](#)
 Headquarters: 45 Beacon Street Boston, MA 02108-3693
 DC Office: 1120 G Street, NW, Suite 800 Washington DC, 20005-3826
amsinfo@ametsoc.org Phone: 617-227-2425 Fax: 617-742-8718
[Allen Press, Inc.](#) assists in the online publication of AMS journals.